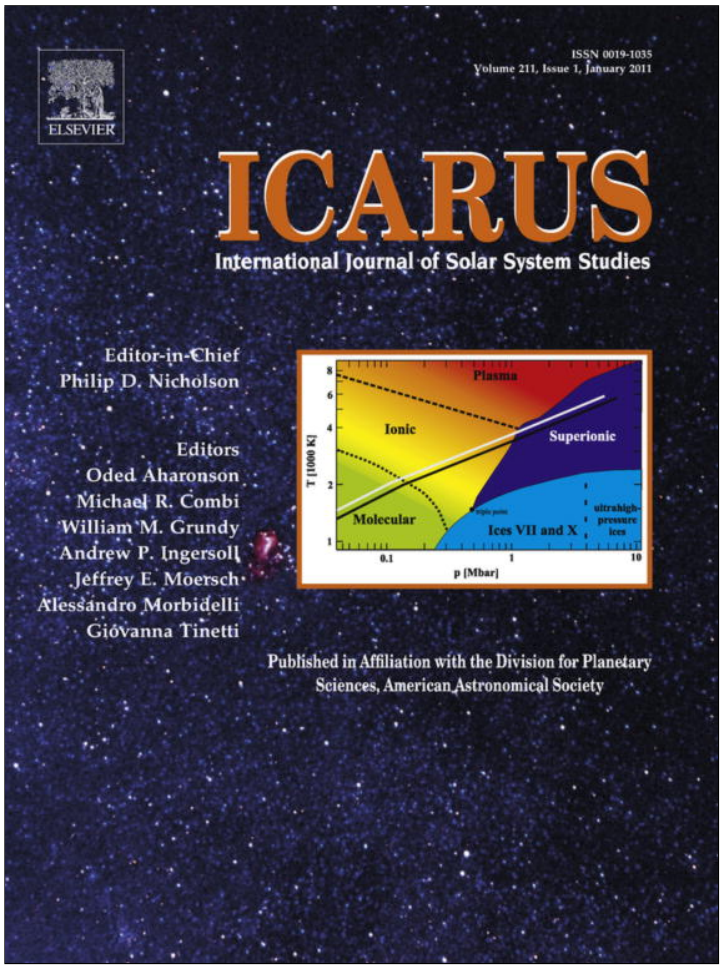

Icarus 211 (2011) 636–647

Contents lists available at ScienceDirect

Icarus

journal homepage: www.elsevier.com/locate/icarus

Strike-slip fault patterns on Europa: Obliquity or polar wander?

Alyssa Rose Rhoden [a,*,1], Terry A. Hurford [b], Michael Manga [a]

[a] University of California at Berkeley, Department of Earth & Planetary Science, Berkeley, CA 94720, United States
[b] NASA Goddard Space Flight Center, Code 693, Greenbelt, MD 20771, United States

ARTICLE INFO

Article history:
Received 24 May 2010
Revised 30 October 2010
Accepted 2 November 2010
Available online 11 November 2010

Keywords:
Europa
Rotational dynamics
Tectonics

ABSTRACT

Variations in diurnal tidal stress due to Europa's eccentric orbit have been considered as the driver of strike-slip motion along pre-existing faults, but obliquity and physical libration have not been taken into account. The first objective of this work is to examine the effects of obliquity on the predicted global pattern of fault slip directions based on a tidal-tectonic formation model. Our second objective is to test the hypothesis that incorporating obliquity can reconcile theory and observations without requiring polar wander, which was previously invoked to explain the mismatch found between the slip directions of 192 faults on Europa and the global pattern predicted using the eccentricity-only model. We compute predictions for individual, observed faults at their current latitude, longitude, and azimuth with four different tidal models: eccentricity only, eccentricity plus obliquity, eccentricity plus physical libration, and a combination of all three effects. We then determine whether longitude migration, presumably due to non-synchronous rotation, is indicated in observed faults by repeating the comparisons with and without obliquity, this time also allowing longitude translation. We find that a tidal model including an obliquity of 1.2°, along with longitude migration, can predict the slip directions of all observed features in the survey. However, all but four faults can be fit with only 1° of obliquity so the value we find may represent the maximum departure from a lower time-averaged obliquity value. Adding physical libration to the obliquity model improves the accuracy of predictions at the current locations of the faults, but fails to predict the slip directions of six faults and requires additional degrees of freedom. The obliquity model with longitude migration is therefore our preferred model. Although the polar wander interpretation cannot be ruled out from these results alone, the obliquity model accounts for all observations with a value consistent with theoretical expectations and cycloid modeling.

1. Introduction

Strike-slip displacement on Europa was first identified by Schenk and McKinnon (1989) within a region of boxy lineaments called "The Wedges". Later, Tufts et al. (1999) identified extensive strike-slip displacement along a cycloid called Astypalaea Linea. The appearance of such strike-slip displacement was puzzling until it was considered within the context of tides. Europa's eccentric orbit leads to daily changes in tidal stress, which may then drive tectonics. Hoppa et al. (1999, 2000) developed a tidal-tectonic model for the formation of strike-slip faults, dubbed "tidal walking", in which tidal stresses acting on a crack lead to net displacement along the crack during each tidal cycle. In particular, throughout an orbit, the tidal stress at a crack cycles through periods of tension, then shear, then compression, and then shear in the opposite direction. Although there are two periods of shear, displacement along the fault mainly occurs while the crack is open; when the crack is closed, friction restricts or even prohibits sliding. The result is a net displacement due to shear stress applied during the open phase (i.e. shear that occurs during a period of tension). Based on this model, the net sense of slip (right or left lateral) along a crack can be predicted if the latitude, longitude, and azimuth of the crack are known. The global pattern of strike-slip motion produced by eccentricity-driven tides has the following characteristics (Hoppa et al., 1999, 2000): only left lateral faults form above 35°N, only right lateral faults form below 35°S, and between these regions, both right and left lateral faults form with the slip-direction depending on the longitude and the azimuth of the crack. A limited survey of strike-slip faults on Europa showed that faults do tend to follow the pattern predicted by the eccentricity-only tidal walking model (Hoppa et al., 2000). In cases where predictions did not match observations, longitudinal displacement, presumably due to non-synchronous rotation, could alleviate the mismatch.

Because Europa's orbit is eccentric, its rotation rate is not constant throughout an orbit. Hence, its spin rate will at times be slower than the rotation rate (i.e. slower than synchronous) and at other times faster, leading to a tidal torque that reduces or increases the spin rate to realign Europa's tidal bulge with the

* Corresponding author.
E-mail address: alyssa@eps.berkeley.edu (A.R. Rhoden).
[1] Previously published under the surname Sarid.

0019-1035/$ - see front matter © 2010 Elsevier Inc. All rights reserved.
doi:10.1016/j.icarus.2010.11.002

direction of Jupiter. Averaged over an orbit, Europa would spin slightly faster than synchronous causing a patch of terrain to migrate eastward relative to the direction of Jupiter as the shell rotates over time (Greenberg and Weidenschilling, 1984). Thus, a set of faults observed at a given longitude on Europa may actually be a combination of faults formed at many different locations relative to Jupiter. Non-synchronous rotation (NSR) is supported by studies of several types of surface features including cycloids and strike-slip faults (McEwen, 1986; Geissler et al., 1998; Hoppa et al., 2001; Kattenhorn, 2002; Hurford et al., 2007; Schenk et al., 2008; see also discussion in Kattenhorn and Hurford (2009) and Bills et al. (2009)). However, rotation of the shell was not detected in a comparison of Voyager and Galileo imagery leading to an estimate of the present-day NSR period of at least 12,000 years (Hoppa et al., 1999b), which could be slow enough that NSR-induced stresses viscously relax and do not contribute to surface stress. In addition, Goldreich and Mitchell (2010) conclude that the stress induced by rotation must be limited to small values for non-synchronous rotation of the ice shell to occur. Hence, NSR may translate features in longitude from their formation locations without significantly altering the stress conditions on the features.

Sarid et al. (2002) conducted a comprehensive mapping of strike-slip faults in the regional mapping imagery taken by the Galileo spacecraft at ~250 m/pixel, which covered two broad swaths extending from about 70°N to 70°S. RegMap02 is in the leading hemisphere, centered at ~80°W and extending about 10° on either side. RegMap01 is in the trailing hemisphere at ~220°W with a southern extension closer to 180°W. They also included a region directly north of RegMap01 that was imaged separately. Examples of faults found in the survey are shown in Fig. 1 from the north trailing hemisphere (Fig. 1a) and south leading hemisphere (Fig. 1b). For each of the 192 mapped faults (Fig. 2 and SOM), Sarid et al. (2002) recorded the latitude, longitude, azimuth, amount of displacement, and sense of slip. To determine whether the strike-slip observations supported the tidal walking model, they used the global predictions of slip direction from Hoppa et al. (1999), which indicated that only left lateral faults form at 45°N and 60°N, only right lateral faults form at 45°S and 60°S, and there is a mixture of right and left lateral faults at intermediate latitudes for which the prediction depends on longitude and crack azimuth. Using these predictions to match specific faults was challenging because the longitudes of the two survey regions fell in between the longitudes at which the predictions were determined (every 30°). There were also many faults with latitudes intermediate to the prediction latitudes. However, relying on only the general pattern, Sarid et al. (2002) showed that the observations and theoretical predictions did not match. In the trailing hemisphere, right lateral faults were observed as far north as 60° and very few left lateral faults were observed just south of the equator. In the leading hemisphere, the mixture of right and left lateral faults extended far south although the number of strike-slip observations in this region was limited due to pervasive chaos.

Sarid et al. (2002) concluded that, based on the general pattern of strike-slip faults expected to form in response to eccentricity-driven tides, ~30° of polar wander had occurred since the majority of the faults formed, causing the pattern to appear too far north in one hemisphere and too far south in the other. In addition, they inferred that polar wander occurred slowly enough that the induced stresses could viscously relax and not impose surface stresses that would otherwise swamp the tidal stress expected to generate these strike-slip faults. The distributions of chaotic terrain and other non-tectonic features also appear to have some oblique antipodal symmetry (Riley et al., 2000; Greenberg et al., 2003) bolstering the polar wander interpretation. If Europa's ice shell is mechanically decoupled from the interior, modest shell thickness variations could induce polar wander. Ojakangas and Stevenson (1989) showed that temperature differences between the equator and poles could lead to thickness variation in the ice shell, and ultimately, reorientation of thicker ice to the equator. However, any process that locally thins the ice shell could theoretically drive polar wander, moving the thinned region poleward.

Since a more detailed comparison was not possible given the sparseness of the predictions, Sarid et al. (2002) did not fully address whether non-synchronous rotation was required to fit the strike-slip observations. However, there was an expectation that any discrepancy between model predictions and observations that was not corrected by polar wander could be accounted for with non-synchronous rotation. In fact, a more detailed comparison using such a model may not offer much additional insight. Polar wander would change the azimuths of displaced faults, in addition to their latitudes, unless the faults happen to fall exactly along the polar wander rotation axis. Determining the extent of azimuth change for a given fault is further complicated if non-synchronous rotation occurs along with slow polar wander thereby moving faults out of alignment over time.

The stress field used to predict these strike-slip patterns incorporated only the tidal effects of Europa's forced eccentricity. Europa's obliquity (the tilt of the spin pole) was expected to be negligibly different from zero due to tidal dissipation. However, Bills (2005) presented a theoretical argument for Europa's obliquity being forced to a non-negligible value due to interactions with the other large satellites of Jupiter. The average obliquity of Europa

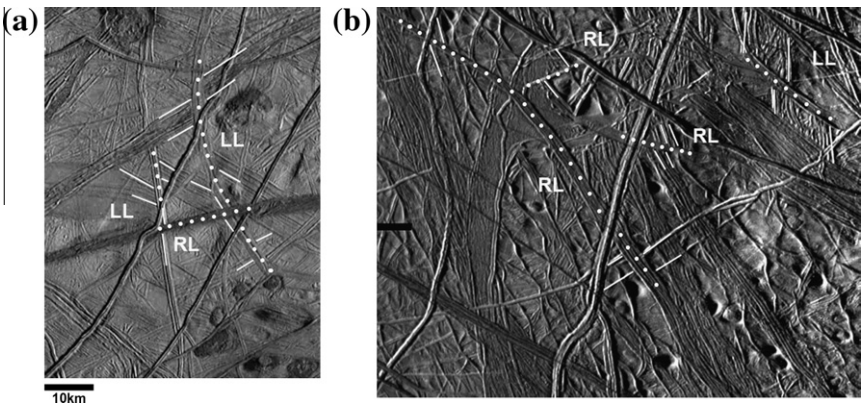

Fig. 1. Examples of strike-slip faults identified in the survey by Sarid et al. (2002) in the (a) north leading hemisphere (orbit e15-01, image s0449961865) and; the scale bar shown applies to both images. White dots trace out the fault along which slip has occurred. Offset features along each fault are highlighted with thin white lines, and the slip direction is noted. Maps of all faults included in the survey are shown in Fig. 1 of Sarid et al. (2002).

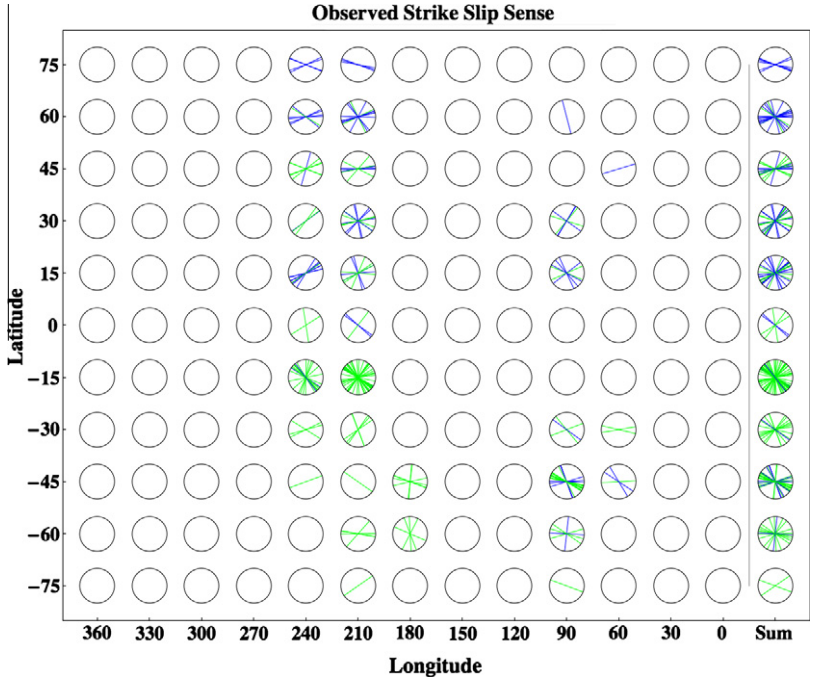

Fig. 2. Observed strike-slip faults from Sarid et al. (2002), binned according to their current latitudes and longitudes for comparison with global predictions. Green lines represent right lateral faults while blue shows left lateral faults. The azimuths of the lines correspond to the azimuths of the faults. At longitude 90° and latitudes 0° and −15°, no faults were mapped due to extensive chaotic terrain. Longitudes that have empty bubbles at all latitudes were not mapped in the strike-slip survey because the image resolution was too low.

would be ~0.1° if the satellite acts as a solid body (Bills, 2005; Bills et al., 2009). The obliquity could be several times larger if the ice shell is mechanically decoupled from the interior. Several lines of evidence point to a global, liquid water ocean under Europa's icy shell (Anderson et al., 1998; Carr et al., 1998; Kivelson et al., 2000), making the decoupled scenario likely. In addition, Europa's obliquity will vary on 10–1000 year timescales (Bills et al., 2009); ~7% variation in the value of Europa's obliquity is expected over geologically relevant timescales if Europa acts as a solid body (Bills, 2005). It is unclear how much the variation in obliquity would increase for a larger average obliquity. Europa's spin pole direction is also expected to precess at a rate of ~0.2–2.21°/day depending again on the interior structure (Bills et al., 2009). Unfortunately, there are few observational constraints on Europa's obliquity, but it is necessarily small to have gone undetected in the gravity measurements (Anderson et al., 1998).

Obliquity causes the latitude of the tidal bulges to vary throughout each Europan day, and hence, alters the pattern of tidal stress. Hurford et al. (2009) investigated the effects of obliquity on the global pattern of cycloids, another proposed tidally-driven feature, because the eccentricity-only model fails to reproduce two important characteristics of observed cycloids. First, a tidal model that incorporates only eccentricity predicts that two regions of boxy cycloids would form on the equator in opposite hemispheres. Although two regions of boxy cycloids are observed, they are offset from the equator – one is too far north, and the other is too far south, but the discrepancy is opposite the offsets in the global strike-slip fault pattern as described by Sarid et al. (2002). The second characteristic that cannot be explained by an eccentricity-only model is the existence of regular cycloids that cross the equator. Hurford et al. (2009) found that, for certain spin pole directions, an obliquity of 0.1° would result in an offset of each boxy region by an amount and in a direction that is consistent with the observations and, in addition, could generate equator-crossing cycloids consistent with those observed. Furthermore, detailed fits to individual cycloids greatly improve when the tidal model includes obliquity (Hurford et al., 2009; Rhoden et al., 2010).

Gravitational torque from Jupiter on the oblate shape of Europa forces a physical libration in addition to the longitudinal libration of the tidal bulges caused by Europa's eccentricity. As with obliquity, the physical libration is typically damped such that its effects are negligible (cf. Peale, 1977). However, Bills et al. (2009) has shown that, if Europa acts as a solid body, physical libration would cause a reference point such as the sub-Jupiter point to undergo longitudinal displacement of ~133 m at the equator, which corresponds to a libration amplitude of 0.005°. The presence of an ocean could increase this value by a factor of 10^3, although the amplification is likely restricted by gravitational coupling between the shell and the interior (see also, Van Hoolst et al., 2008). We have been unable to identify any observational constraints on Europa's libration in the literature.

Using various tidal stress models to fit individual cycloids, both at the equator and in the southern hemisphere, Rhoden et al. (2010) found evidence of a variable obliquity averaging ~1° as well as large and variable physical libration. Specifically, the obliquities ranged from 0.32° to 1.35°, and the libration amplitudes varied from 0.72° to 2.44°. The libration phases mainly clustered between −6.04° and 17.72°. These findings are consistent with the theoretical predictions in the case that Europa has a subsurface ocean separating the ice shell from the interior. There was almost no signal of fast spin pole precession within cycloid shapes, suggesting that either precession is slower than expected or cycloid formation is not sensitive to small changes in spin pole direction. Stress from non-synchronous rotation (NSR) did little to improve cycloid fits although longitude translation, presumably due to NSR, was required to obtain good fits with all models (Rhoden et al., 2010).

Here, we investigate the influence of obliquity on fault slip direction and reevaluate the polar wander interpretation of observed strike-slip faults. We first update the global predictions from Hoppa et al. (1999, 2000), which incorporated only eccentricity, because

the predictions for the region in which both right and left lateral faults can form were incorrect (Section 3.1, Appendix A). We next produce global predictions that incorporate obliquity. Finally, we predict the slip direction for each strike-slip fault recorded by Sarid et al. (2002) using tidal models with and without obliquity, physical libration, and longitude migration. Consistent with theoretical expectations and results from our previous cycloid modeling (Rhoden et al., 2010), we find that a tidal model including obliquity of at least 1.2°, along with longitude migration, can predict the slip directions of all observed features in the survey. Adding physical libration to the obliquity model increases the number of correctly predicted features at their current longitudes, but cannot account for all observations. Applying a tidal model that incorporates obliquity alleviates the need to invoke polar wander in order to reconcile the tidal walking hypothesis with observations, although both scenarios require longitude migration presumably due to non-synchronous rotation.

2. Methodology

In the tidal walking hypothesis, daily changes in tidal stress control the opening and closing of pre-existing faults at the surface and the direction of the net shear displacement along the faults. To calculate tidal stress, we use the equations for the principal stresses in a thin, relative to radius, elastic shell for a radially symmetric body (e.g., Melosh, 1977, 1980):

$$\sigma_\delta = C(5 + 3\cos 2\delta_P) \tag{1a}$$
$$\sigma_\alpha = -C(1 - 9\cos 2\delta_P) \tag{1b}$$

where $C = 3h_2M\mu(1+\nu)/8\pi\rho a^3(5+\nu)$ and h_2 is the tidal Love number, M is Jupiter's mass, μ is the shear modulus, ν is Poisson's ratio, ρ is the average density, a is the distance between Jupiter and Europa, and δ_P is the angular distance from a point on Europa's surface to the primary tidal bulge. The σ_δ stress is directed radially from the tidal bulges and the σ_α stress is perpendicular to σ_δ. The third principal stress is negligible in a shell that is thin relative to radius. Since all the stress calculations contain a factor of C, its value does not influence our results.

Europa's eccentricity causes the tidal bulges to librate in longitude while obliquity predominantly causes a latitudinal libration. Spherical trigonometry is used to calculate the varying location of the tidal bulge, which depends on the spin pole direction and the true anomaly. Since the locations of the tidal bulges are changing, the angular distance to the bulge, δ, also changes. The tidal stress equations can thus be modified to account for the eccentricity and obliquity (Hurford et al., 2009; Rhoden et al., 2010).

$$\sigma_\delta = C(1 - e\cos n)^{-3}(5 + 3\cos 2\delta) \tag{2a}$$
$$\sigma_\alpha = -C(1 - e\cos n)^{-3}(1 - 9\cos 2\delta) \tag{2b}$$

and

$$\text{bulge colatitude} = \pi/2 - \varepsilon\sin(n + \varphi) \tag{2c}$$
$$\text{bulge longitude} = -2e\sin n \tag{2d}$$

where e is eccentricity, ε is obliquity, φ is the spin pole direction (SPD), and n is the true anomaly. When Europa is at pericenter, if the spin pole is pointing toward Jupiter, the SPD is defined as 90°; SPD increases clockwise. Stress from the diurnal tide can be calculated by subtracting the primary tidal stress (Eqs. (1a) and (1b)) from the stress due to eccentricity and obliquity (Eqs. (2a) and (2b)) once both stresses have been rotated to a common coordinate system. The resulting diurnal stresses are $\sigma_{\delta*}$ in the direction of the north pole, and the perpendicular stress is $\sigma_{\alpha*}$. The last step is to decompose the diurnal tidal stress into normal and shear components relative to a fault's orientation, where z is the azimuth of the crack measured clockwise from north.

$$\sigma_n = 0.5(\sigma_{\delta*} + \sigma_{\alpha*}) + 0.5(\sigma_{\delta*} - \sigma_{\alpha*})\cos(2\zeta) + \sigma_{\delta\alpha}\sin(2\zeta) \tag{3a}$$
$$\sigma_\tau = -0.5(\sigma_{\delta*} - \sigma_{\alpha*})\sin(2\zeta) + \sigma_{\delta\alpha}\cos(2\zeta) \tag{3b}$$

Whereas eccentricity causes the tidal bulges to move relative to a fixed reference location such as the sub-Jupiter point, physical libration is the oscillation of that reference point. The motion is caused by gravitational torques from Jupiter on Europa's oblate figure and is characterized by an amplitude, α, and a phase, ϕ. A libration phase of 0° indicates that the reference line is tracking the tidal bulge; a 180° phase means the reference line is moving in the opposite direction of the tidal bulge. Libration enters the tidal stress equations in the bulge longitude calculation. Eq. (2d) becomes:

$$\text{bulge longitude} = -2e\sin(n) + \alpha\sin(n + \phi) \tag{3}$$

We first focus on the effects of obliquity, to determine if the latitudinal variation in bulge location caused by obliquity can account for the latitudinal mismatch between theory and observations. We then add longitude translation or physical libration to determine whether either motion improves the predictions. We do not include any stress from non-synchronous rotation or polar wander when determining predictions of slip direction. In addition, we do not address the formation mechanism of the pre-existing crack, only subsequent motion along the fault.

To determine the slip direction along a fault, we first specify the latitude and longitude of the fault, the fault azimuth, and the amount of obliquity and spin pole direction (SPD). There is degeneracy between spin pole direction and longitude such that the stress field is identical when both are modulated by 180°. Using these parameters, we calculate the stress throughout an orbit, beginning at pericenter and ending at apocenter. We then evaluate the changes in stress over time using a tidal walking model to determine the prediction for slip direction along the fault.

Fig. 3 shows the normal and shear stresses plotted over one orbit for a fault with azimuth 120° at a longitude of 210° in the far north (Fig. 3a) and far south (Fig. 3b). When the normal stress changes from negative (compression) to positive (tension), shear displacement along the crack is encouraged. This corresponds to the "opening" phase described by Hoppa et al. (1999, 2000). However, as long as slip can occur more easily during the tensile phase than during the compressive phase, the tidal walking model should still produce displacement even without physically opening the crack. The time at which this transition occurs is marked A in Fig. 3a, and corresponds to a near maximum in right lateral shear stress, resulting in an initial right lateral displacement, which then decreases over time until switching to left lateral shear (point B).

Because the local region of interest is connected to Europa's global ice shell, we conceptualize the sides of the fracture as two ice blocks pinned far from the location of the fracture. As the blocks distort under the influence of tidal shear stress, there is a competing elastic restoring force due to the ice shell's elasticity. Thus, as the right lateral shear stress decreases, the displacement on the fault also decreases (Fig. 3a). When the shear stress reaches zero, at point B, we would expect no displacement along the crack due to the elastic response of the shell. After point B, and until the fault closes (point C), the shear stress is increasingly left lateral. Therefore, we would predict left lateral displacement along this northern hemisphere fault during the open phase. The opposite is true in the southern hemisphere (Fig. 3b) in which, after opening occurs, the left lateral shear stress decreases and then becomes increasingly right lateral resulting in a right lateral fault. We can, therefore, use the shear direction at the time of closing to predict the slip direction along the fault. Although we treat the ice shell as elastic,

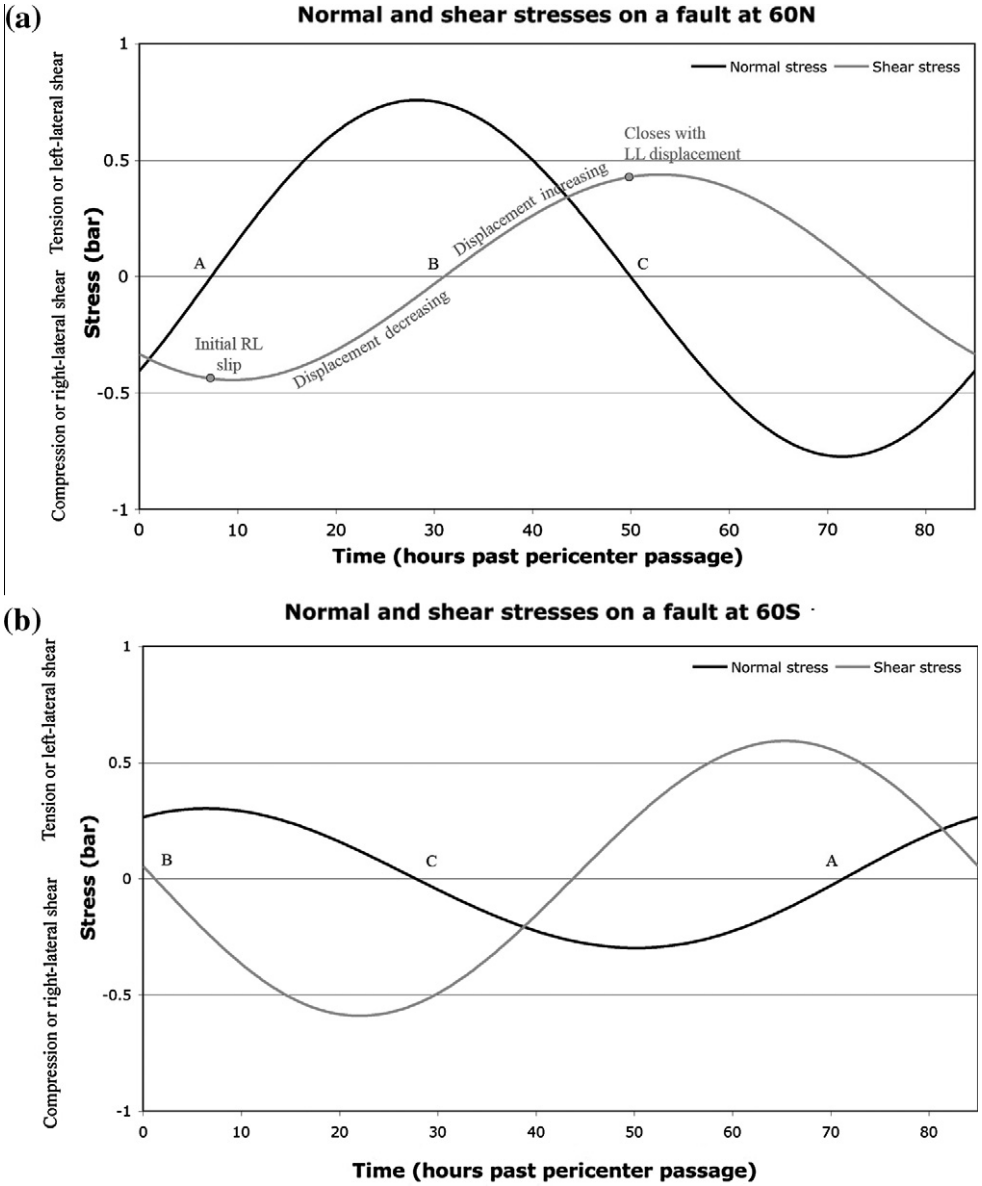

Fig. 3. Stress change throughout one orbit on a fault of azimuth 120° at longitude 210° and latitude 60°N (a) or 60°S (b). The normal stress is shown in black, and the shear stress is gray. In the tidal walking theory, shear occurs more easily when the normal stress becomes tensile (i.e. greater than 0), which occurs at A, than when the normal stress becomes compressive, at point C. Between these times, the shear stress controls the displacement along the fault. The point at which the shear stress switches from decreasing right lateral to increasing left lateral (in case a; the opposite for case b) is marked as B. Since the northern fault (a) is subject to left lateral shear when the fault becomes compressive, it would exhibit left lateral displacement. The southern fault (b) should then be right lateral.

which is probably appropriate at the surface when subjected to daily-varying stress, the tidal walking model assumes that some stress is slowly relaxed during the dormant phase causing the fault to retain a net displacement in each subsequent orbit (Hoppa et al., 1999, 2000).

3. Results

3.1. Global strike-slip predictions

To examine the influence of obliquity on global strike-slip patterns, we determined the slip directions of hypothetical faults at azimuths from 0° to 180° in increments of 1°, for every 30° of longitude, and every 15° of latitude from 75°N to 75°S; we tested obliquity values of 0°, 0.5°, and 1.0° with spin pole directions of 0°, 90°, 180°, and 270°. If Europa's spin pole precesses quickly with respect to the accumulation of strike-slip displacement along faults, the fault displacements in the survey may reflect different spin pole directions. We therefore also computed the predictions for spin pole directions at every 30° combined. Finally, we examined the potential effects of longitude migration due to non-synchronous rotation by combining predictions at all longitudes.

Fig. 4 shows the global predictions for the eccentricity-only case (see also, Appendix A). Black represents fault azimuths that undergo left lateral slip, light gray represents right lateral slip, and white shows cases where no net slip is predicted. The white regions are difficult to discern since the prediction of no net slip tends to apply just at the azimuth separating predictions of right and left lateral fault motion. At the equator, these regions are slightly more visible and run nearly horizontal and nearly vertical. The last column of Fig. 4 shows a combination of the predictions made at each

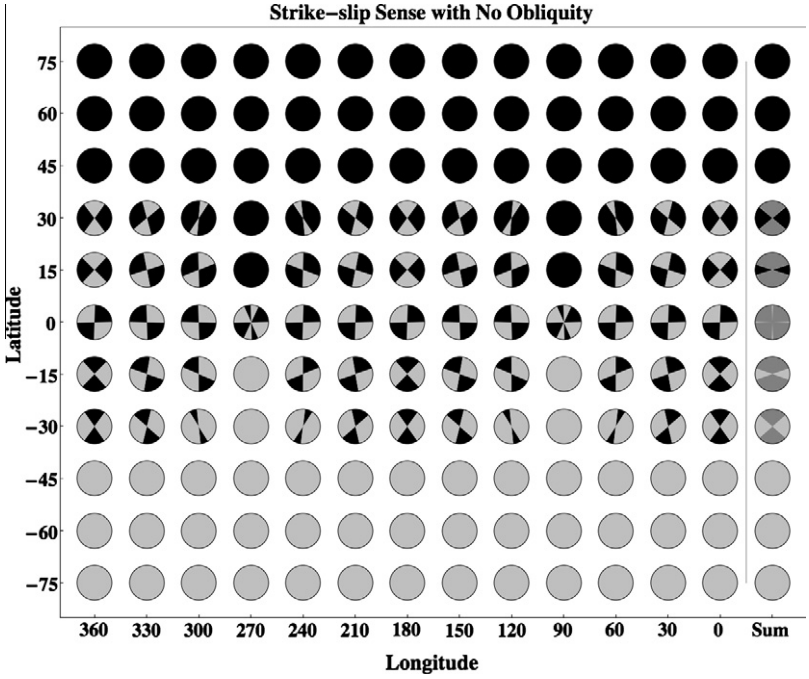

Fig. 4. Predictions with zero obliquity. Within each circle, black regions indicate crack azimuths along which we predict left lateral displacement; light gray represents right lateral fault azimuths, and white indicates that no net slip is predicted. The last column shows the predictions summed over all longitudes, in which dark gray represents azimuths that could have right or left lateral displacement depending on their longitude at the time the displacement occurred.

longitude. Here, dark gray indicates that both right and left lateral faults form within the span of longitudes tested for a given crack azimuth. The overall pattern we find is the same as Hoppa et al. (1999). In the region of mixed right and left lateral faults, our predictions differ because Hoppa et al. (1999) incorrectly decomposed stresses along the crack when making their predictions. This error would probably not have changed the interpretation by Sarid et al. (2002) since it was based on the global pattern, but it would affect a more detailed analysis of near-equatorial faults (such as our analysis, described in Section 3.2).

Fig. 5 shows the global predictions for an obliquity of 1.0°, at each of the four SPDs (a–d) and for SPDs at every 30° combined (e). Plots using an obliquity of 0.5° can be found in the SOM. The last column of each plot shows the predictions combined over all longitudes. Just as before, black signifies left lateral faults, light gray signifies right lateral faults, dark gray indicates that either type of fault can form, and white shows cases where we predict no net slip. These global prediction plots show that increasing obliquity creates increasing asymmetry in the fault pattern. Right lateral faults can form in the far north, left lateral faults can form in the far south, and the mixed regions are offset from the equator in different patterns depending on the spin pole direction. Considering these global prediction plots, it seems plausible that the observed pattern of strike-slip faults (Fig. 2) may be accounted for by inclusion of obliquity.

3.2. Direct comparison to observed faults

We conducted a direct comparison between our predictions and the 192 observed strike-slip faults from Sarid et al. (2002). To do this, we used the exact locations of the faults rather than the global prediction grid. Sarid et al. (2002) showed maps of strike-slip faults they identified; the corresponding database of faults contains the azimuth, slip direction, and latitude and longitude for the starting and ending points of each fault (SOM). We checked the database against Galileo images that have been tied into Europa's latitude/longitude grid (image cubes were obtained from the Planetary Image Research Lab at University of Arizona) and found that the latitude information for many faults in the leading hemisphere appeared incorrect. Further investigation revealed that latitude information in the Galileo regional mosaics (e.g. E17REGMAP01) differs from that of the global mosaics in which Galileo images are inset into global Voyager imagery. In regions that were imaged by Voyager and included in the Galileo regional mapping data set, the latitudes were again inconsistent although resolution may also be an issue in those cases. Latitudes vary by as much as 1° in the southern leading hemisphere, which also causes some variability in the corresponding longitudes of affected features. In regions where both right and left lateral faults can form, the azimuth cutoff between the two may change slightly depending on the latitude and longitude. Because of the uncertainties in location and ambiguity as to where along each fault to make the comparison, we made predictions at all of the points listed as starting points and then at all of the ending points (SOM). We conducted tests to determine the extent to which the uncertainty in location influenced our results. Using models that do not include longitude migration, we found that the predictions differ for 0–2 faults depending on the exact location at which the prediction is made. In cases where the results were different, we report the higher number of incorrectly predicted faults. With longitude migration, the accuracy of the longitude measurement is less important because the prediction will not be made at that longitude.

Using the current fault locations (SOM), we tested tidal models with eccentricity only, eccentricity and obliquity, eccentricity and physical libration, and all three effects combined. The values of obliquity we tested were guided by which global predictions had asymmetric patterns consistent with observations. In addition, we tested physical libration amplitudes of 0.5°, 1.0°, and 1.5° using libration phases of 0°, 90°, 180°, and 270°. For our final test, we added longitude migration to the eccentricity-only and obliquity models by making predictions at every 10° of longitude. In cases with longitude migration, we considered a fault to be accurately predicted if its slip direction was matched at any tested longitude. Results from our comparisons with observed faults are

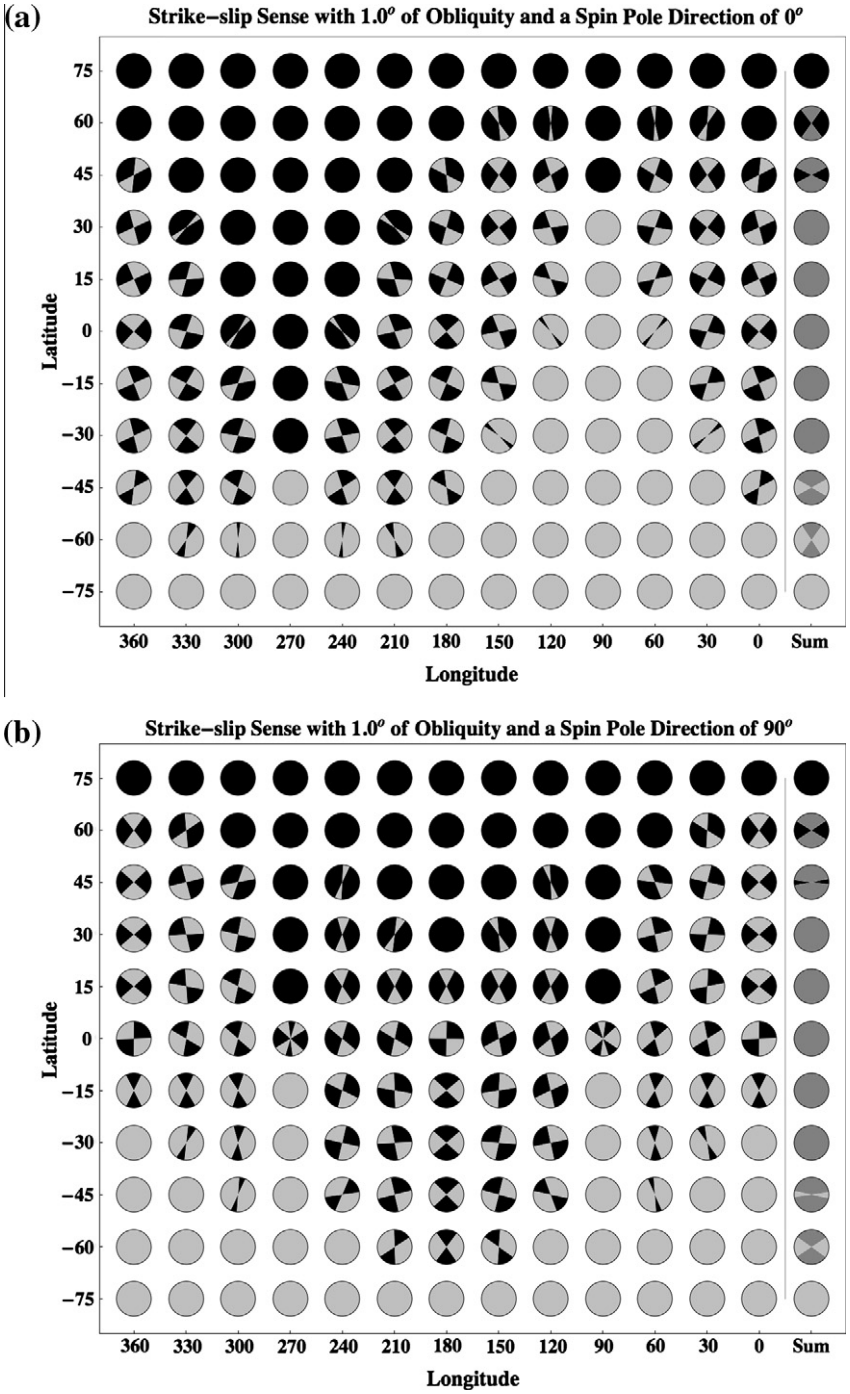

Fig. 5. (a–e) Predictions with 1.0° obliquity at spin pole directions of 0° (a), 90° (b), 180° (c), 270° (d), and with SPDs at every 30° combined (e). In each plot, the last column shows the predictions at all longitudes combined. Black represents fault azimuths that will exhibit left lateral displacement, and light gray represents right lateral faults; dark gray indicates that either type of fault can form, and white shows cases where we do not predict any net slip.

summarized in Table 1 in which we list each of the models tested and the number of features that could not be produced with each model.

Using the current locations of the faults, the eccentricity-only model fails to predict the slip directions of 71 faults. Adding physical libration (without obliquity) does not improve the results for any combination of libration amplitude or phase we tested. The global predictions show that an obliquity less than 1° produces strike-slip patterns that are not asymmetric enough to match the observed strike-slip patterns so we explored values between 1° and 1.2°. The best of these tidal models includes an obliquity of 1.0° with SPD 270°, and still cannot fit 60 faults. With all SPDs combined, the lowest number of mismatched faults falls to 27 with 1.2° of obliquity.

In our last attempt to predict faults at their current locations, we use a tidal model that combines 1.2° of obliquity, the combined predictions at spin pole directions every 30°, and physical libration. Using a libration amplitude of 1° and libration phase of 0° provides the best match to observations, accurately predicting all but six faults. Although this result requires no longitude migration, the model does introduce additional degrees of freedom from the libration amplitude and phase and requires the assumption of fast

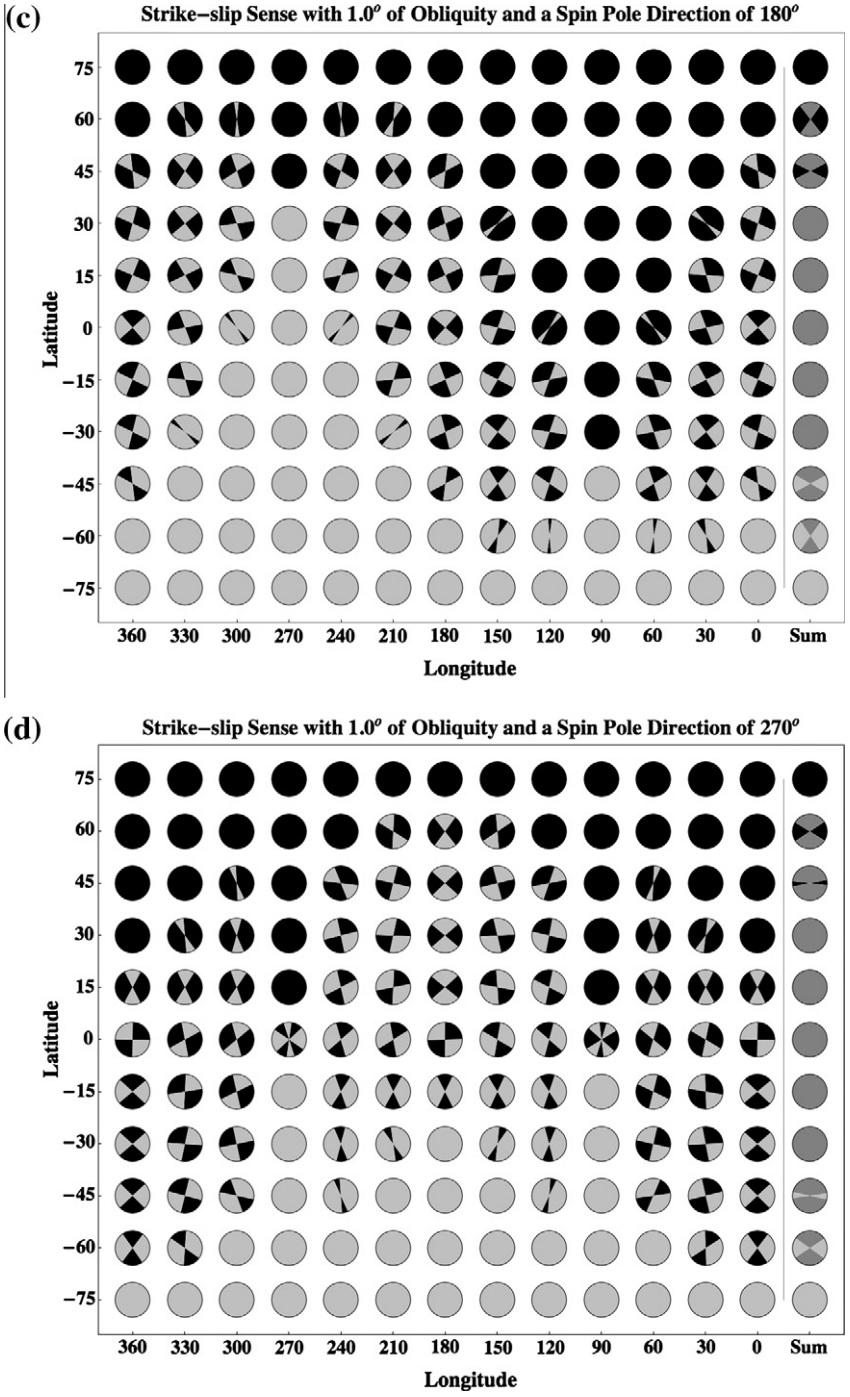

Fig. 5 (*continued*)

spin pole precession to justify combining predictions made with different spin pole directions.

Allowing longitude migration improves results for the eccentricity-only and obliquity cases. We did not test any tidal models that included physical libration or combined spin pole directions along with longitude migration. The predictions using the eccentricity-only model match all but 30 faults. An obliquity of 1° and a spin pole direction of 90° (equivalent to 270°) combined with longitude migration can accurately predict the slip directions of all but four faults. Increasing the obliquity to 1.1° fits all but one fault; 1.2° results in accurate predictions for the slip directions of all 192 faults.

4. Discussion

We used a modified version of the tidal walking model to predict slip direction, based on the direction of shear stress at the time the normal stress becomes compressive. Hoppa et al. (1999, 2000) used the difference in shear stress at opening versus closing. If the shear stress increased while the crack was open (i.e. in tension), they predicted left lateral displacement; a decrease resulted in right lateral displacement. In cases where the magnitude of the shear stress was the same at opening and closing, they predicted no slip on the fault. The only substantial differences between these two methods are in the predictions at the equator, which Hoppa

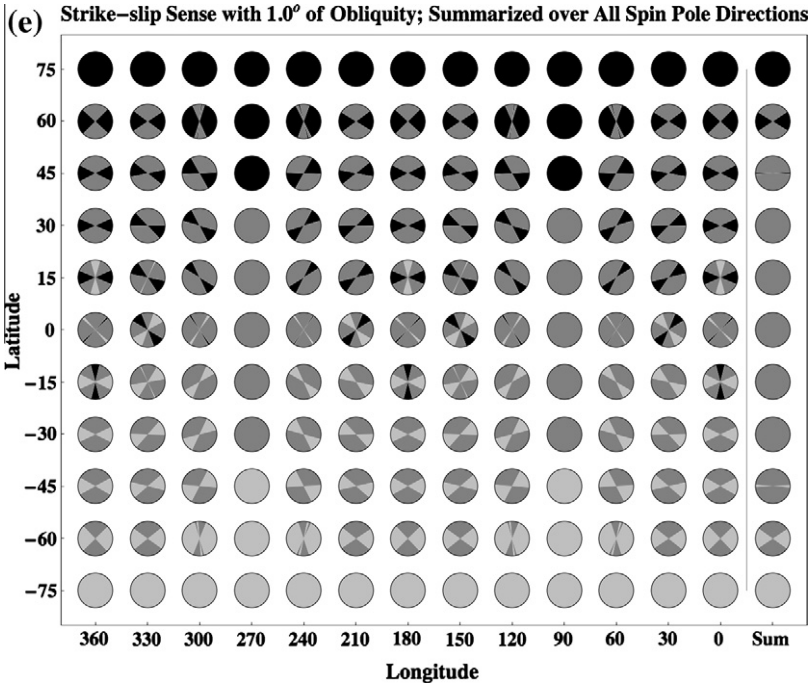

Fig. 5 (*continued*)

Table 1
Tidal models tested against strike-slip observations and corresponding results.

Obliquity (°)	Spin pole direction	Longitude migration	Physical libration amplitude (°)	Physical libration phase	Number of incorrectly predicted faults
0		No	0		71
0		No	0.5	Any	71
0		No	1.0	Any	71
0		No	1.5	90°/180°/270°	71
1	270°	No	0		60
1.1	270°	No	0		63
1.2	270°	No	0		63
1	Combined	No	0		30
1.1	Combined	No	0		28
1.2	Combined	No	0		27
1.2	Combined	No	0.5	0°	18
1.2	Combined	No	1.0	0°	6
1.2	Combined	No	1.5	90°	18
0		Yes	0		30
1	90°/270°	Yes	0		4
1.1	90°/270°	Yes	0		1
1.2	90°/270°	Yes	0		0

et al. (1999, 2000) did not show in their global prediction plots. We attempted to fit observed strike-slip faults using both methods in test cases with and without obliquity, libration, and longitude migration; the results differed for 1–2 faults in several cases. However, we also tested those cases that provided the best fit to observed faults and found no difference in the number of faults fit with each method.

Our global predictions (Figs. 4 and 5) show systematic changes in the predicted slip directions of faults from exclusively left lateral in the far north to only right lateral in the far south for most longitudes. However, in Fig. 4, 5b, and 5d, the equatorial predictions at longitudes 90° and 270° have a unique pattern with additional disconnected regions in which right or left lateral faults form. Upon further inspection of the stress in this region, we found that the magnitude of the normal stress is much less than the shear stress, which could permit shear displacement along the fault even when it is in compression contrary to the "rules" of the tidal walking model. This would result in a prediction of no net slip rather than right or left lateral. We should note that Sarid et al. (2002) did not identify any faults in these regions due to low-resolution imagery (at 270°) and the prevalence of chaotic terrain (at 90°) so the ambiguity in model prediction does not affect our results and can not be assessed by comparison with observation. Nonetheless, this case highlights the major shortcoming of the tidal walking model: its lack of a detailed mechanical treatment of slip along the faults.

For this work, applying the tidal walking model was necessary because we are reassessing previous conclusions made using that model in light of the new evidence for non-negligible obliquity. In addition, tidal walking is the only model that has been shown to reproduce the global pattern of strike-slip observations. However, a strike-slip model for Enceladus' tiger stripes has been proposed (Smith-Konter and Pappalardo, 2008), which employs a Coulomb failure criterion to determine if and when faults will slip and a linear elastic relationship between stress and strain to quantify the net slip on faults. Since no evidence of strike-slip displacement has been observed along the tiger stripes, the model has not

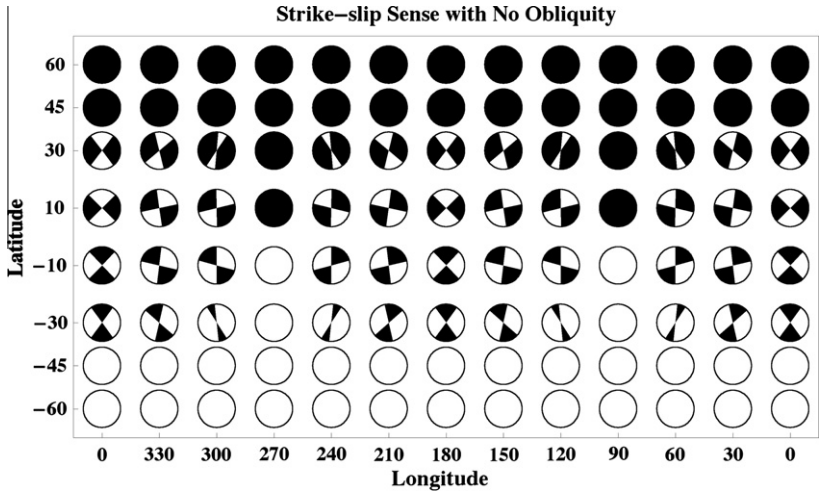

Fig. A1. Predictions with zero obliquity using the same latitude/longitude grid, prediction method, and color scheme as Hoppa et al. (1999, 2000). Here, black is left lateral, but white is right lateral. Our revised predictions do not display the pinwheel character seen in the original Hoppa predictions. Comparison with Fig. 3 confirms that the different prediction methods have little influence on the predictions.

yet been validated. A useful direction for additional work on Europa's strike-slip faults would be to incorporate a more detailed mechanical treatment of slip along faults, perhaps akin to that of Smith-Konter and Pappalardo (2008), into the tidal walking model. Such a model could be vetted in a similar manner to our current assessment, by testing its ability to generate the observed global pattern of strike-slip faults on Europa. In addition, the magnitude of displacements may also be useful for testing models that include a more mechanical treatment.

Kattenhorn (2004) identified some faults with strike-slip displacement that also display sharp kinks or veers, similar to terrestrial tailcracks in which the veers or kinks form in response to slip on the original fault. By comparing the geometries of the tailcracks to predictions based on linear elastic fracture mechanics, Kattenhorn (2004) concluded that the "ridge-like" strike-slip faults displaying tailcracks formed without a significant dilational component. In other words, the displacements occurred when the fault was in compression, which is contrary to the tidal walking model. "Band-like" strike-slip faults with tailcracks were found to be consistent with tidal walking. As previously discussed, expanding the tidal walking model to allow for slip during compression would be more realistic and could perhaps explain the formation of the "ridge"-like tailcrack faults. In addition, it is certainly plausible that some strike-slip faults on Europa are formed through a different process than tidal walking or even due to regional rather than tidal stresses. Inadvertently including some of these features in our analysis could impede our ability to match fault statistics with our various tidal models. However, given the large number of observed faults (192) compared to the seven "ridge-like" faults with tailcracks identified by Kattenhorn (2004), it is unlikely to have significantly impacted our results.

We find that an obliquity of 1.2°, with longitude migration, can match all the observations in the Sarid et al. (2002) database. However, the obliquity is predicted to change on timescales that are short relative to Europa's surface age (Bills et al., 2009) so the tectonic record likely includes features formed with different obliquity values. Therefore, we consider 1.2° to be the maximum obliquity indicated by strike-slip faults; the average value could be much lower and still account for strike-slip observations. These results are consistent with theoretical expectations (Bills et al., 2009) and results from cycloid modeling (Hurford et al., 2009; Rhoden et al., 2010). Although we cannot rule out the slow polar wander hypothesis previously invoked to explain observations of strike-slip faults on Europa (Sarid et al., 2002), we find it unnecessary in light of the mounting tectonic evidence in favor of obliquity (Bills et al., 2009; Hurford et al., 2009; Rhoden et al., 2010).

The implications for physical libration are not obvious. The model that includes both obliquity and physical libration is successful at fitting all but six faults at their current locations, but adding longitude migration to the obliquity model accounts for all strike-slip observations with fewer free parameters. This implies that, at least statistically, longitude migration is the more robust model. Studies of cycloids, however, support both physical libration and longitude migration due to non-synchronous rotation (e.g. Rhoden et al., 2010). Perhaps, when additional imagery allows for a more extensive survey of strike-slip faults, we can distinguish between these two effects and determine if there is a signal of physical libration in strike-slip patterns. Alternatively, if Europa's physical libration is a large as cycloid modeling indicates (~1°), it may be measurable using Earth-based radar techniques (e.g. Margot et al., 2007).

Our conclusion that the "offsets" in Europa's strike-slip fault patterns are not the result of slow reorientation but rather are the result of obliquity, does not rule out the possibility of other polar wander events throughout Europa's history. Semi-circular depressions and trough systems observed in both hemispheres of Europa are thought to be among the remnants of an ~80° polar wander event (Schenk et al., 2008). These features presumably formed in response to the large stresses incurred by polar wander. These stresses should also have generated extensive strike-slip faulting, but such features have not yet been identified (Schenk et al., 2008) perhaps because they were overprinted by subsequent tectonic activity. Polar wander stress was also proposed to influence the formation of global-scale lineaments, but comparison between observed lineament azimuths and theoretical predictions were not definitive (Leith and McKinnon, 1996). In short, our results are not in conflict with the formation of semi-circular depressions via polar wander.

One of the distinguishing characteristics of the strike-slip observations is that they exhibit a different pattern in one hemisphere than the other: the region of mixed right and left lateral faults extends north of the equator in the trailing hemisphere and south of the equator in the leading hemisphere. That is what led to the polar wander interpretation and our interest in applying obliquity to the predictions. When we sum the predictions over all longitudes, this piece of information is obscured. It appears, from looking at the

sum columns in Fig. 5a–e that, with enough obliquity, almost any pattern of strike-slip motion could be fit once we allow longitude migration. However, we find that only limited longitude shift is required to match the vast majority of the slip directions of faults when obliquity is included in the tidal model. Specifically, using 1.2° of obliquity and a phase of 90°, we accurately predict over 90% of the fault motions with no more than 90° of longitude migration (assuming no NSR stress accumulation). Obliquity produces the hemispheric pattern required to fit most of the observations with limited longitude shift. Summing over all longitudes allows us to also account for the few remaining outliers, which may be older slip events in the record. Lineament sequences have been established in many regions of Europa (e.g. Sarid et al., 2004), which could perhaps be used to test the hypothesis that faults requiring more longitude migration are in fact older.

The existence of the observed hemispheric pattern may also have implications for the amount and rate of NSR reflected in the tectonic record even though we do not incorporate stress from the rotation in our tidal models. The lack of mixed right and left lateral faults in the south trailing hemisphere, for example, suggests that the most recent tectonic record does not include longitudes at which mixed faults form. However, 180° away from the current longitudes, the obliquity model would produce a mixture of faults south of the equator. This suggests that the majority of fault motions in the record occurred within the last 180° of NSR (we find <90° is sufficient for most faults), and that the rate of strike-slip displacement was fast compared to the NSR rate. Conversely, if NSR was fast with respect to the formation of these faults, the pattern should be roughly the same at all longitudes: a wider band of mixed faults extending equally far both north and south of the equator.

The implication that only a fraction of a rotation has occurred in recent Europan history is quite different from the results of in-depth analyses of lineaments and cycloids (see also Kattenhorn and Hurford, 2009). Geissler et al. (1998) first suggested that the azimuths of lineaments should change systematically (increasing clockwise in the north and counter-clockwise in the south) as the surface rotates non-synchronously through the stress field. Their initial finding, based on cross-cutting relationships mapped in low-resolution imagery, found evidence of the expected pattern with time and determined that much less than one rotation was reflected in the azimuths. However, subsequent analysis (Sarid et al., 2005), which relied on higher resolution imagery and included many more lineaments and cross-cutting relationships, found that there was no pattern; the lineament azimuths in the region were indistinguishable from a random set. The lineament azimuths may in fact be changing systematically with time, but the lack of NSR signal suggests that lineament formation is slow with respect to the rate of NSR such that too few lineaments form per cycle to display a continuous pattern. If the prescribed pattern were applied, a minimum of one but generally several non-synchronous cycles would be required to account for the lineament azimuths in the regional mapping areas (Figueredo and Greeley, 2000; Sarid et al., 2004, 2005, 2006) and the "bright plains" equatorial region (Kattenhorn, 2002). Modeling of cycloids (Hoppa et al., 2001; Hurford et al., 2009; Rhoden et al., 2010) and the average orientations of cycloids (Groenleer and Kattenhorn, 2008) also suggest greater than one and up to several non-synchronous rotations of the surface. However, cycloids are less numerous than lineaments and often do not have as many useful cross-cutting relationships that can be used to create long time sequences.

Despite the apparent contradiction, the results from studies of strike-slip faults and lineament azimuths may be consistent. The lineaments in a given region may in fact form slowly with respect to NSR such that many rotations of the surface are reflected in their azimuths. Then, subsequent strike-slip motion could occur along the lineaments – a process that could be fast with respect to NSR. The result of these two processes could be a set of lineaments with little signal of NSR but exhibiting strike-slip motion with a very strong signal that reflects activity mainly during the past 90–180° of rotation. For this idea to be viable, older strike-slip motion would need to be largely erased such that the strike-slip record is constantly being reset. Rapid resurfacing would eliminate the older slip record but would also eliminate the lineaments, which do appear to be preserved over several rotations. Alternatively, strike-slip motion along a fault in one direction could perhaps be erased by subsequent motion in the opposite direction as stresses change due to longitude migration. Developing a mechanical model to explore this hypothesis would be an interesting avenue of future work.

A more complex tidal model will also affect the expected lineament azimuth patterns. Geissler et al. (1998) made their predictions of systematic azimuth change based on non-synchronous rotation through an eccentricity-generated tidal stress field. Perhaps the azimuths would not follow such a simple pattern if obliquity and/or physical libration were included in the model of tidal stress. In that case, the lineament azimuths could potentially reflect much less rotation than otherwise indicated and be more consistent with the strike-slip record.

The implications for NSR depend mostly on our ability to sample both north and south of the equator. Therefore, sampling bias should not be an issue for the trailing hemisphere where we have the same amount and quality of imagery from about 75°N to 75°S. The observation that the mixed region is north of the expected location based on the eccentricity model, and the far south has little to no mixing should not be the result of observation bias. In the leading hemisphere, there is extensive chaotic terrain just south of the equator, which did result in gaps in the observations. In Fig. 2, the empty circles at longitude 90° and latitudes 0° and −15° reflect areas that could not be mapped due to chaos (whereas the additional empty circles represent regions that were not mapped by Sarid et al. (2002) due to a lack of high-resolution imagery). Regardless, even further south where chaos is not an issue, both right and left lateral faults were observed that cannot be explained without obliquity even with longitude migration.

5. Conclusions

By incorporating an obliquity of 1.2°, we find that a tidal walking formation model combined with subsequent non-synchronous rotation can correctly predict the sense of slip of all the observed faults. Slow polar wander, invoked by Sarid et al. (2002) to explain the latitudinal mismatch between strike-slip predictions and observations, is no longer necessary once the effects of obliquity are included. Obliquity has also been shown to alleviate mismatches between cycloid formation models and observations, which polar wander would not directly resolve. Slow non-synchronous rotation is indicated within the strike-slip record, but the majority of fault motions require limited rotation. This suggests that the majority of the observed strike-slip occurred in only a fraction of a non-synchronous rotation of the surface, and thus, occurs quickly with respect to NSR. Measuring Europa's current obliquity, spin pole direction, and physical libration would be useful goals of any future mission.

Acknowledgments

The authors wish to thank E.M. Huff and B. Militzer for several helpful discussions and the NAI and NESSF programs for funding this work.

Appendix A

In Fig. 4, we show revised predictions for slip direction without obliquity on a finer grid than was presented in Hoppa et al. (1999, 2000) and using our criteria for determining slip direction. For more direct comparison, we show the predictions at the same grid points and using the original criteria in Fig. A1. Note that here we follow the convention of Hoppa et al. (1999, 2000), using white rather than light gray to represent right lateral faults. The difference between our predictions and the Hoppa predictions is most obvious in the pinwheel character seen at 10°S and 10°N, which was apparently an artifact of applying vector decomposition to the total stress tensor when determining the normal and shear components relative to a fault. In addition, comparison with Fig. 4 shows that there is no significant difference between the two methods for predicting slip direction.

Appendix B. Supplementary material

Supplementary data associated with this article can be found, in the online version, at doi:10.1016/j.icarus.2010.11.002.

References

Anderson, J.D., Schubert, G., Jacobson, R.A., Lau, E.L., Moore, W.B., Sjogren, W.L., 1998. Europa's differentiated internal structure: Inferences from four Galileo encounters. Science 281, 2019–2022.

Bills, B.G., 2005. Free and forced obliquities of the Galilean satellites of Jupiter. Icarus 175, 233–247.

Bills, B.G., Nimmo, F., Karatekin, O., Van Hoolst, T., Rambaux, N., Levrard, B., Laskar, J., 2009. Rotational dynamics of Europa. In: Pappalardo, R., McKinnon, W., Khurana, K. (Eds.), Europa. Univ. Arizona Press, Tucson, pp. 119–136.

Carr, M.H. et al., 1998. Evidence for a subsurface ocean at Europa. Nature 391, 363–365.

Figueredo, P.H., Greeley, R., 2000. Geologic mapping of the northern leading hemisphere of Europa from Galileo solid-state imaging data. J. Geophys. Res. 105, 22629–22646.

Geissler, P.E. et al., 1998. Evolution of lineaments on Europa: Clues from Galileo multispectral imaging observations. Icarus 135, 107–126.

Goldreich, P.M., Mitchell, J.L., 2010. Elastic shells of synchronously rotating Moons: Implications for cracks on Europa and non-synchronous rotation on Titan. Icarus 209, 631–638. doi:10.1016/j.icarus.2010.04.013.

Greenberg, R., Leake, M.A., Hoppa, G.V., Tufts, B.R., 2003. Pits and uplifts on Europa. Icarus 161, 102–126.

Greenberg, R., Weidenschilling, S.J., 1984. How fast do Galilean satellites spin? Icarus 58, 186–196.

Groenleer, J., Kattenhorn, S.A., 2008. Cycloid crack sequences on Europa: Relationship to stress history and constraints on growth mechanics based on cusp angles. Icarus 193, 158–181.

Hoppa, G.V., Tufts, B.R., Greenberg, R., Geissler, P., 1999. Strike-slip faults on Europa: Global shear patterns driven by tidal stress. Icarus 141, 287–298.

Hoppa, G., Greenberg, R., Tufts, B.R., Geissler, P., Phillips, C., Milazzo, M., 2000. Distribution of strike-slip faults on Europa. J. Geophys. Res. 105, 22617–22627.

Hoppa, G.V., Tufts, B.R., Greenberg, R., Hurford, T.A., O'Brien, D.P., Geissler, P.E., 2001. Europa's rate of rotation derived from the tectonic sequence in the Astypalaea region. Icarus 153, 208–213.

Hurford, T.A., Sarid, A.R., Greenberg, R., 2007. Cycloidal cracks on Europa: Improved modeling and non-synchronous rotation implications. Icarus 186, 218–233.

Hurford, T.A., Sarid, A.R., Greenberg, R., Bills, B.G., 2009. The influence of obliquity on Europan cycloid formation. Icarus 202, 197–215.

Kattenhorn, S.A., 2002. Nonsynchronous rotation evidence and fracture history in the Bright Plains region, Europa. Icarus 157, 490–506.

Kattenhorn, S.A., 2004. Strike-slip fault evolution on Europa: Evidence from tailcrack geometries. Icarus 172, 582–602.

Kattenhorn, S.A., Hurford, T., 2009. Tectonics on Europa. In: Pappalardo, R., McKinnon, W., Khurana, K. (Eds.), Europa. Univ. Arizona Press, Tucson, pp. 199–236.

Kivelson, M.G., Khurana, K.K., Russell, C.T., Volwerk, M., Walker, M., Walker, R.J., Zimmer, C., 2000. Galileo magnetometer measurements: A stronger case for a subsurface ocean at Europa. Science 289, 1340–1343.

Leith, A.C., McKinnon, W.B., 1996. Is there evidence for polar wander on Europa? Icarus 120, 387–398.

Margot, J.L., Peale, S.J., Jurgens, R.F., Slade, M.A., Holin, I.V., 2007. Large longitude libration of Mercury reveals a molten core. Science 316, 710–714.

McEwen, A.S., 1986. Tidal reorientation and the fracturing of Jupiter's moon Europa. Nature 321, 49–51.

Melosh, H.J., 1977. Global tectonics of a despun planet. Icarus 31, 221–243.

Melosh, H.J., 1980. Tectonic patterns on a tidally distorted planet. Icarus 43, 334–337.

Ojakangas, G.W., Stevenson, D.J., 1989. Polar wander of an ice shell on Europa. Icarus 81, 242–270.

Peale, S.J., 1977. Orbital resonances in the Solar System. Annu. Rev. Astron. Astrophys. 14, 215–246.

Rhoden, A.R., Militzer, B., Huff, E.M., Hurford, T.A., Manga, M., Richards, M., 2010. Constraints on Europa's rotational dynamics from modeling of tidally-driven fractures. Icarus 210, 770–784. doi:10.1016/j.icarus.2010.07.018.

Riley, J., Hoppa, G.V., Greenberg, R., Tufts, B.R., Geissler, P., 2000. Distribution of chaotic terrain on Europa. J. Geophys. Res. – Planets 105, 22599–22615.

Sarid, A.R., Greenberg, R., Hoppa, G.V., Hurford, T.A., Tufts, B.R., Geissler, P., 2002. Polar wander and surface convergence of Europa's ice shell: Evidence from a survey of strike-slip displacement. Icarus 158, 24–41.

Sarid, A.R., Greenberg, R., Hoppa, G.V., Geissler, P., Preblich, B., 2004. Crack azimuths on Europa: Time sequence in the southern leading face. Icarus 168, 144–157.

Sarid, A.R., Greenberg, R., Hoppa, G.V., Brown Jr., D.M., Geissler, P., 2005. Crack azimuths on Europa: The G1 lineament sequence revisited. Icarus 173, 469–479.

Sarid, A.R., Greenberg, R., Hurford, T.A., 2006. Crack azimuths on Europa: Sequencing of the northern leading hemisphere. J. Geophys. Res. 111, E08004. doi:10.1029/2005JE002524.

Schenk, P., McKinnon, W.B., 1989. Fault offsets and lateral crustal movement on Europa: Evidence for a mobile ice shell. Icarus 79, 75–100.

Schenk, P., Matsuyama, I., Nimmo, F., 2008. True polar wander on Europa from global-scale small-circle depressions. Nature 453, 368–371.

Smith-Konter, B., Pappalardo, R.T., 2008. Tidally driven stress accumulation and shear failure of Enceladus' tiger stripes. Icarus 198, 435–451.

Tufts, B.R., Greenberg, R., Hoppa, G.V., Geissler, P., 1999. Astypalaea Linea: A San Andreas-sized strike-slip fault on Europa. Icarus 141, 53–64.

Van Hoolst, T., Rambaux, N., Karatekin, Oe., Dehant, V., Rivoldini, A., 2008. The librations, shape, and icy shell of Europa. Icarus 195, 386–399.